JOURNAL OF SOLID STATE CHEMISTRY 118, 313–322 (1995)

A Survey of Superstructures in Intermetallic NiAs–Ni_2In-Type Phases

Sven Lidin and Ann-Kristin Larsson

Department of Inorganic Chemistry 2, Lund University, P.O. Box 124, S-221 00 Lund, Sweden

Received November 21, 1994; in revised form February 13, 1995; accepted February 15, 1995

This survey covers the NiAs–Ni_2In-type structures and ordered superstructures in the *T–B* systems. Only compounds with a *c/a* value between 1.2 and 1.3 are treated. Twenty-three reports of superstructures were found, exhibiting 16 different unit cells; 14 of these structures are reported as solved and they form 11 distinct structure types. © 1995 Academic Press, Inc.

INTRODUCTION

The *B*8-type structures, NiAs ($B8_1$) and Ni_2In ($B8_2$), are very common indeed in *T–B* systems, with *T* being a transition metal and *B* a chalcogenide, a pnictide, or an element from the boron or carbon group. The structures are simple; the symmetry is $P6_3/mmc$ and the *B* atom is in Wyckoff position 2*c* (1/3 2/3 1/4), forming a hexagonal close-packed array, while the *T* atom is in 2*a* (0 0 0), filling all the octahedral interstices. In $B8_2$ the extra *T* atom is in position 2*d* (1/3 2/3 3/4), filling the trigonal bipyramidal interstices of the B-atom array. These positions will henceforth be referred to by their respective Wyckoff symbols, *a*, *c*, and *d*. The distinction between $B8_1$ and $B8_2$ is rather vague since nonstoichiometry is rampant in these systems and the structure types are often used interchangeably. To complicate matters further, the nonstoichiometry tends to yield superstructure ordering.

There is an important distinction that may be made on the basis of the *c/a* ratio of *B*8 alone. At high values of *c/a* (1.4–2.0) the tendency is for compounds to exhibit a 1 : 1 stoichiometry or a *B*-rich composition such as Cr_2S_3 ($c/a = 1.62$) and Co_2Te_3 ($c/a = 1.40$). The nonstoichiometry is here caused by partial occupancy of the octahedral interstices. At lower *c/a* values (1.2–1.3) compounds tend to be *T*-rich. It is convenient to use the hybrid term $B8_1$–$B8_2$ for compounds with a composition between *TB* and T_2B and a structure generated by the ordered partial occupancy of the positions corresponding to 2(*d*) NiAs. The term *B*8 will be used for compounds with the simple NiAs or Ni_2In in the compound, with low values for metallic bonding and higher values indicating increasing ionicity. This survey deals with *B*8 compounds of metallic character in the lower *c/a* range. The aim of the survey is to identify the superstructures and incompletely known phases of the $B8_1$–$B8_2$ structure type reported and to suggest likely candidates for further study.

BINARY *T–B B*8 STRUCTURES

For each *B* element we have surveyed the literature, concentrating on pure *B*8 and superstructures caused by the ordered partial occupancy of position 2(*d*) ($B8_1$–$B8_2$). All structure variants not strictly *B*8 or $B8_1$–$B8_2$ were excluded. There is a host of closely related structures such as Mn_5Si_3, Sn_5Ti_6, Ga_4Ti_5, Fe_3Sn_2, and CoGe, where different vacancy patterns, interleaved layers of Laves-type phases, substitutions of single atoms for groups of atoms, and crystallographic shear and slip break the strict $B8_1$–$B8_2$ nature of the structure. Since the superstructures may take on virtually any symmetry, the search was based on composition only. The search includes data from three different compilations: Pearson's Handbook (1), Hansen's Constitution of Binary Alloys (2), and the Powder Diffraction File (3). Among the pnictides and chalcogenides, antimony alone yields transition metal compounds in the required *c/a* range (1.2–1.3). Compounds in that range with elements in the boron and carbon group are legion, with the only exception being boron (BPt and BRh are reverse $B8_1$) and carbon (no *B*8 structure compounds) themselves. For each reported compound the primary method used for the determination of unit cell, symmetry, and structure (when applicable) is quoted under the heading "data." PXRD and SXRD denote X-ray powder diffraction and single crystal X-ray studies, while SAED stands for selected area electron diffraction. The matrices of transformation from the B8 cell are found in Appendix A.

The Boron Group

Aluminum. Three *B*8 structures are reported in the systems Al–*T*: Al_2Cu_3, $AlSc_2$, and $AlZr_2$. Additionally, two superstructures of Al–Cu have been reported; Al_2Cu_3 with doubled *c*- and *a*-axes, and the monoclinic form Al_9Cu_{12} with a cell given by matrix M_2.

0022-4596/95 $12.00

Compound	a(Å)	b(Å)	c(Å)	β	matrix	ref.	data	spacegroup	
Al_2Cu_3	4.146	4.146	5.063	---	I	4	PXRD	$P6_3/mmc$	(194)
Al_2Cu_3	8.09	8.09	9.99	---	M_1	5	PXRD	Orthorhombic	
Al_9Cu_{12}	7.07	4.08	10.02	90.63	M_2	6	PXRD	Monoclinic	
$AlSc_2$	4.888	4.888	6.166	---	I	7	SXRD	$P6_3/mmc$	(194)
$AlZr_2$	4.894	4.894	5.928	---	I	8	PXRD	$P6_3/mmc$	(194)

Gallium. Two *B*8 type structure systems are reported: $GaTi_2$ and $GaNi_2$. In the Ni system the compositions Ga_2Ni_3 and $Ga_{41}Ni_{59}$ are given as well. The latter composition is given for a monoclinic cell (In_3Pt_4 type) compatible with the transformation matrix M_3.

Compound	a(Å)	b(Å)	c(Å)	β	matrix	ref.	data	spacegroup	
$GaNi_2$	4.002	4.002	4.988	---	I	9,10	PXRD	$P6_3/mmc$	(194)
$Ga_{41}Ni_{59}$	13.822	7.894	8.478	35.8	M_3	9,11	PXRD	C2/m	(12)
$GaTi_2$	4.51	4.51	5.50	---	I	12	PXRD	$P6_3/mmc$	(194)

Indium. Indium forms *B*8- and $B8_1$–$B8_2$-type structures with Ni, Cu, Sc, and Pt. The system Ni–In contains the phases $InNi_2$, In_2Ni_3, and $In_{21}Ni_{29}$. The $In_{21}Ni_{29}$ phase has the In_3Pt_4-type structure, while the structure of In_2Ni_3 is unknown. Its cell is given by the transformation matrix M_2. The only *B*8 type structure in the In–Pt system is the In_3Pt_4 structure type, while in the In–Cu system there are reports of no less than three phases of the composition $Cu_{16}In_9$; one simple *B*8 structure, and two orthorhombic phases with cells given by the transformation matrices M_4 and M_5. $InSc_2$ is reported as a simple *B*8 structure.

Compound	a(Å)	b(Å)	c(Å)	β	matrix	ref.	data	spacegroup	
$InNi_2$	4.179	4.179	5.131	---	I	13,14	PXRD	$P6_3/mmc$	(194)
In_2Ni_3	7.40	4.26	10.46	---	M_2	15	PXRD	$P2_1$ or $P2_1/m$	
$In_{21}Ni_{29}$	14.646	8.329	8.977	35.35	M_3	11	PXRD	C2/m	(12)
In_3Pt_4	15.338	8.802	9.439	36.11	M_3	11,16	PXRD	C2/m	(12)
ht-$Cu_{16}In_9$	34.194	7.395	5.262	---	M_4	17	PXRD	Orthorhombic	
lt-$Cu_{16}In_9$	21.375	7.405	5.218	---	M_5	17	PXRD	Orthorhombic	
$InSc_2$	5.02	5.02	6.25	---	I	18	PXRD	$P6_3/mmc$	(194)

Thallium. Ni and Pd form *B*8 structures with Tl. The Ni–Tl system contains only one known *B*8 phase, NiTl. The Pd–Tl system is more complex with regard to the $B8_1$–$B8_2$-type structures. The phase Pd_2Tl is reported as basic *B*8, while $Pd_{13}Tl_9$ is a hexagonal-type structure with a doubling of the *a*-axis.

Compound	a(Å)	b(Å)	c(Å)	β	matrix	ref.	data	spacegroup	
NiTl	4.426	4.426	5.535	---	I	19,20	PXRD	$P6_3/mmc$	(194)
Pd_2Tl	4.54	4.54	5.67	---	I	21	PXRD	$P6_3/mmc$	(194)
$Pd_{13}Tl_9$	8.958	8.958	5.623	---	M_6	22	SXRD	$P\bar{3}m1$	(156)

The Carbon Group

Silicon. There are two known *B*8-type compounds with silicon: Rh_3Si_2 and Ir_3Si_2. Both are reported as simple *B*8 structures.

Compound	a(Å)	b(Å)	c(Å)	β	matrix	ref.	data	spacegroup	
Rh_3Si_2	3.949	3.949	5.047	---	I	23	PXRD	$P6_3/mmc$	(194)
Ir_3Si_2	3.963	3.963	5.126	---	I	23	PXRD	$P6_3/mmc$	(194)

Germanium. The Ge–*T* systems are rich in *B*8 phases. They are found in systems with Mn, Fe, Co, and Ni. Superstructures of the $B8_1$–$B8_2$-type have been reported in the Ge–Fe and Ge–Ni systems.

Compound	a(Å)	b(Å)	c(Å)	β	matrix	ref.	data	spacegroup	
Co_3Ge_2	3.933	3.933	5.014	---	I	13	PXRD	$P6_3/mmc$	(194)
Fe_3Ge_2	3.998	3.998	5.010	---	I	24	PXRD	$P6_3/mmc$	(194)
$Fe_{13}Ge_8$	7.976	7.976	4.993	---	M_6	24	PXRD	$P6_3/mmc$	(194)
$GeMn_2$	4.171	4.171	5.278	---	I	25	PXRD	$P6_3/mmc$	(194)
Ge_4Ni_7	3.937	3.937	5.078	---	I	26	PXRD	$P6_3/mmc$	(194)
$GeNi_2$	10.13	7.80	6.83	90.4	M_7	27	SXRD	C2/m	(12)
$Ge_{12}Ni_{19}$	11.631	6.715	10.048	90.0	M_8	26	PXRD	C2	(5)
Ge_3Ni_5	11.682	6.737	6.264	52.11	M_9	26	SXRD	C2	(5)

Tin. Tin forms the largest number of *B*8 structures of all the *B* elements. Likewise, its structural diversity is unparalleled. *B*8 structures in the *c*/*a* range 1.2–1.3 are formed with Ti, Mn, Fe, Co, Ni, CuRh, Pd, and Au. Superstructures are reported with Co, Cu, Mn, Ni, and Pd.

Compound	a(Å)	b(Å)	c(Å)	β	matrix	ref.	data	spacegroup	
AuSn	4.3218	4.3218	5.523	---	I	28	SXRD	$P6_3/mmc$	(194)
Co_3Sn_2	4.109	4.109	5.180	---	I	9,29	PXRD	$P6_3/mmc$	(194)
Co_3Sn_2	7.089	5.221	8.198	---	M_{10}	30	SXRD	Pnma	(62)
Co_3Sn_2	16.445	16.445	5.179	---	M_{11}	31	PXRD	Hexagonal	
η'-Cu_6Sn_5	11.036	7.288	9.841	98.81	M_{12}	32	SAED	C2/c	(15)
η^6-Cu_5Sn_4	9.83	7.27	9.83	62.5	M_{13}	33	SAED	$P2_1/c$	(14)
η^6-Cu_5Sn_4	12.60	7.27	10.20	90.0	M_6	33	SAED	C2	(5)
$Fe_{13}Sn_{10}$	4.216	4.216	5.244	---	I	34	PXRD	$P6_3/mmc$	(194)
MnSn	4.370	4.370	5.475	---	I	35	PXRD	$P6_3/mmc$	(194)
MnSn	13.194	13.194	5.616	---	M_{14}	35	PXRD	Hexagonal	
Ni_3Sn_2	4.125	4.125	5.198	---	I	9	PXRD	$P6_3/mmc$	(194)
Ni_3Sn_2	7.11	5.21	8.23	---	M_{10}	15	SXRD	Pnma	(62)
Pd_3Sn_2	4.399	4.399	5.666	---	I	36	PXRD	$P6_3/mmc$	(194)
$Pd_{20}Sn_{13}$	8.7985	8.7985	16.9837	---	M_{15}	37	PXRD	$P3_121$	(152)
Rh_3Sn_2	4.340	4.340	5.553	---	I	38	PXRD	$P6_3/mmc$	(194)
$SnTi_2$	4.653	4.653	5.700	---	I	39	PXRD	$P6_3/mmc$	(194)

Lead. The Pb–Pd system is *B*8 phase-rich, and has been studied in great detail. Two $B8_1$–$B8_2$ superstructures have been reported. The systems with Ni, Pt, and Rh contain only one known *B*8-type phase each.

Compound	a(Å)	b(Å)	c(Å)	β	matrix	ref.	data	spacegroup	
NiPb	4.15	4.15	5.28	---	I	40	PXRD	$P6_3/mmc$	(194)
Pb_9Pd_{13}	4.493	4.493	5.762	---	I	41,42	PXRD	$P6_3/mmc$	(194)
Pb_9Pd_{13}	15.6027	9.0599	13.911	55.88	M_{16}	41	SXRD	C2/c	(15)
Pb_3Pd_5	13.331	7.667	7.258	52.22	M_9	42	PXRD	Monoclinic	
PbPt	4.259	4.259	5.467	---	I	36	PXRD	$P6_3/mmc$	(194)
Pb_2Rh_3	4.330	4.330	5.639	---	I	43	PXRD	$P6_3/mmc$	(194)

The Pnictides

Antimony. The only transition metal pnictides that form *B*8 structures in the required *c*/*a* range (1.2–1.3) are the antimonides with Nb, Fe, and V and the bismuthide BiPt. They are all reported to form the simple *B*8 structure.

Compound	a(Å)	b(Å)	c(Å)	β	matrix	ref.	data	spacegroup	
NbSb	4.270	4.270	5.447	---	I	44	PXRD	$P6_3/mmc$	(194)
Fe_3Sb_2	4.132	4.132	5.175	---	I	9,45	PXRD	$P6_3/mmc$	(194)
Sb_2V_3	4.285	4.285	5.44	---	I	46,47	PXRD	$P6_3/mmc$	(194)
BiPt	4.324	4.324	5.501	---	I	48	PXRD	$P6_3/mmc$	(194)

The bismuth-based systems contain a number of phases (BiMn, Bi_3Pd_5, Bi_2Pt_3) that are *B*8-type superstructures, but their *c*/*a* ratios are just above 1.3.

SUPERSTRUCTURES

The presence and nature of the superstructures are hard to ascertain by macroscopic methods alone. Even when elucidated superstructures are nonhexagonal, the deviation of the unit cell from hexagonal is slight, if detectable at all. This leads to domain twinning, yielding diffraction patterns with perfect hexagonal intensity distributions. Small domains often lead to X-ray superstructure reflections that are diffuse and weak and selected area electron diffraction should be used as a standard procedure in these systems to reveal the unit cell of single domains. Literature data from XRD studies alone should be treated with caution, and even single crystal X-ray structure determinations are uncertain if film methods are not used and refinement has not been pursued to high accuracy.

In all, 23 examples of superstructures of the $B8_1$–$B8_2$-type were found in the literature, which exhibited 16 distinct cells. The cells were checked for uniqueness by three criteria: the determinant of the transformation matrix, the length of the *c*-axis, and the symmetry of the cell. Some of these structures have been solved, or been assigned to reasonable structural proposals, while others are only known in terms of their cells. A total of 11 different structure types have been reported for the $B8_1$–$B8_2$-type superstructures; see Figs. 1–11. It may be noted that the structure type for $Pd_{20}Sn_{13}$ is $Ga_3Ge_6Ni_{12}$, a ternary compound not treated in this survey.

Compound	Structure	Coordinate table entry	Matrix
Al_2Cu_3	Unknown	-----	M_1
Al_5Cu_{12}	Unknown	-----	M_2
$Ga_{41}Ni_{59}$	In_3Pt_4	1	M_3
In_2Ni_3	Unknown	-----	M_2
$In_{21}Ni_{29}$	In_3Pt_4	1	M_3
In_3Pt_4	Type structure	1	M_3
ht-$Cu_{16}In_9$	Unknown	-----	M_4
lt-$Cu_{16}In_9$	Unknown	-----	M_5
$Pd_{13}Tl_9$	Type structure	2	M_6
$Fe_{13}Ge_8$	Type structure	3	M_6
$GeNi_2$	Unknown	-----	M_7
$Ge_{12}Ni_{19}$	Type structure	4	M_8
Ge_3Ni_5	Type structure	5	M_9
Co_3Sn_2	Ni_3Sn_2	6	M_{10}
Co_3Sn_2	Unknown	-----	M_{11}
η'-Cu_6Sn_5	Type structure	7	M_{12}
η^8-Cu_5Sn_4	Type structure	8	M_{13}
η^6-Cu_5Sn_4	Type structure	9	M_6
MnSn	Unknown	-----	M_{14}
Ni_3Sn_2	Type structure	6	M_{10}
$Pd_{20}Sn_{13}$	$Ga_3Ge_6Ni_{12}$	10	M_{15}
Pb_9Pd_{13}	Type structure	11	M_{16}
Pb_3Pd_5	Unknown	-----	M_9

In the coordinate tables the following information is given: the atomic species, the Wyckoff position and its point group symmetry, the fractional coordinates, the occupancy, the corresponding Wyckoff position in the base cell and the ideal values of the fractional coordinates as calculated from the base cell via the transformation matrix, and finally the contribution from that atom to the occupancy in the base cell. This last piece of information shows whether there are any vacancies in the *B*8 lattice. The accumulated occupancy of the base cell is given in the footnote of the table. In the table heading, the space group, the origin shift in the transformed cell from the *B*8 origin, and the size of the cell are given. Below each coordinate table, the idealized structure (corresponding to the second set of coordinates in the table) is shown. For clarity, only the atoms corresponding to the 2*d* positions in *B*8 are plotted. The background 6^3-net shows the basic

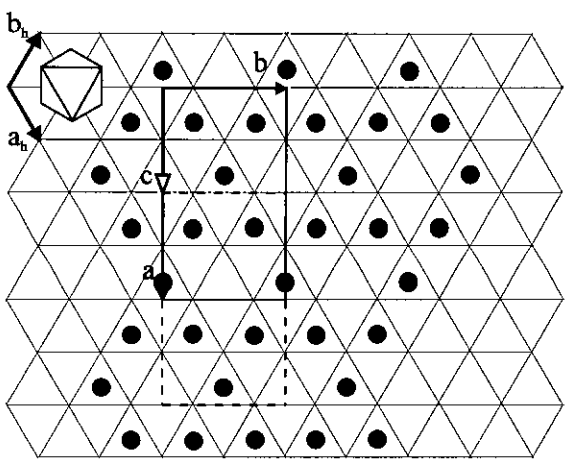

FIG. 1. Pt_4In_3, bounded projection along 001*. The repeat distance along the *c*-axis in *B*8 is doubled. The occupied positions corresponding to 2*d* in $B8_1$–$B8_2$ form Kagomé nets at four different heights; 1/4, 3/4, 5/4, 7/4, in units of the *B*8 *c*-axis.

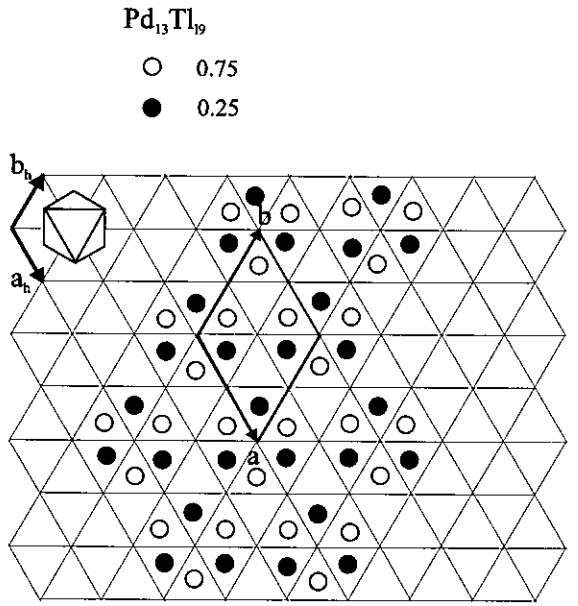

FIG. 2. $Pd_{13}Tl_9$, projection along 001*. The occupied positions corresponding to 2*d* in $B8_1$–$B8_2$ form Kagomé nets at the heights 1/4 and 3/4 in units of the *B*8 *c* axis.

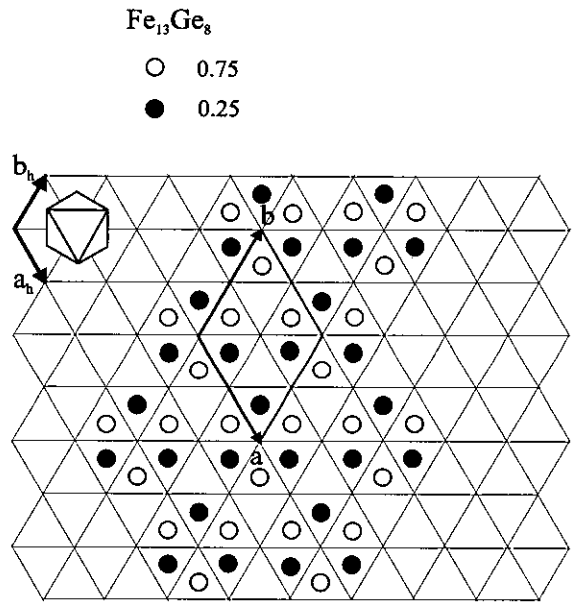

FIG. 3. $Fe_{13}Ge_9$, projection along 001*. The occupied positions corresponding to 2*d* in $B8_1$–$B8_2$ form Kagomé nets at the heights 1/4 and 3/4 in units of the *B*8 *c*-axis.

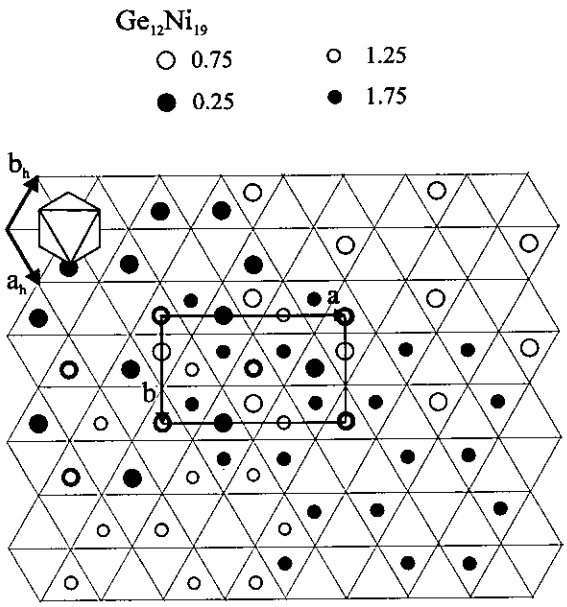

FIG. 4. $Ge_{12}Ni_{19}$, projection along 001*. The repeat distance along the c-axis in $B8$ is doubled. The occupied positions corresponding to $2d$ in $B8_1$–$B8_2$ form 6_3-nets at the heights 1/4, 5/4, 7/4, and a 3_6-net at 3/4 in units of the $B8$ c axis.

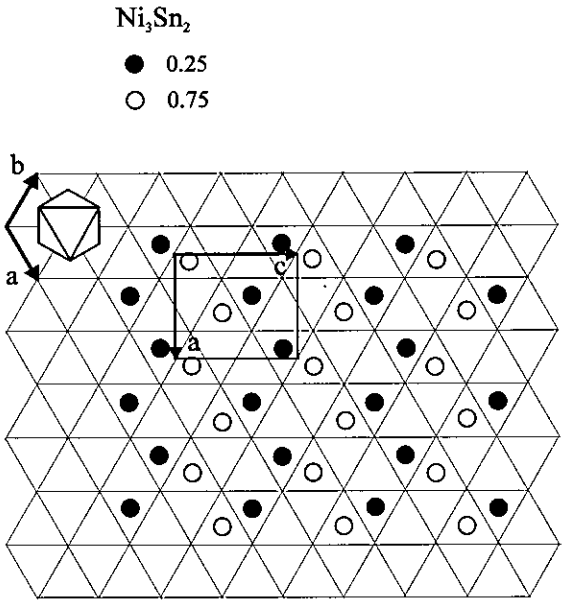

FIG. 6. Ni_3Sn_2, projection along 010*. The occupied positions corresponding to $2d$ in $B8_1$–$B8_2$ form zigzag lines along the orthorhombic c-axis at the heights 1/4 and 3/4 in units of the $B8$ c axis.

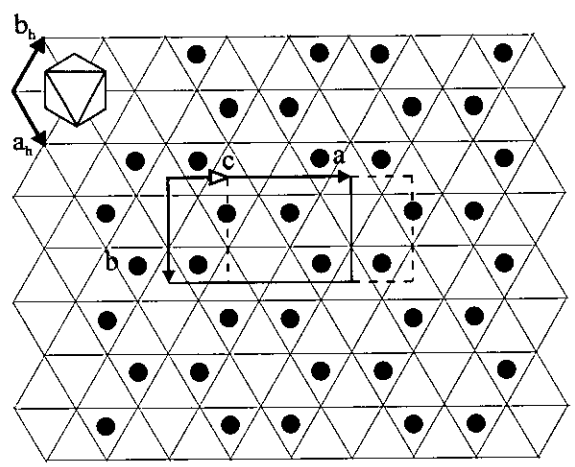

FIG. 5. Ge_3Ni_5, bounded projection along 001*. The repeat distance along the c-axis in $B8$ is tripled. The occupied positions corresponding to $2d$ in $B8_1$–$B8_2$ form 6_3-nets at the heights 1/4, 3/4, 5/4, 7/4, 9/4, and 11/4 in units of the $B8$ c axis.

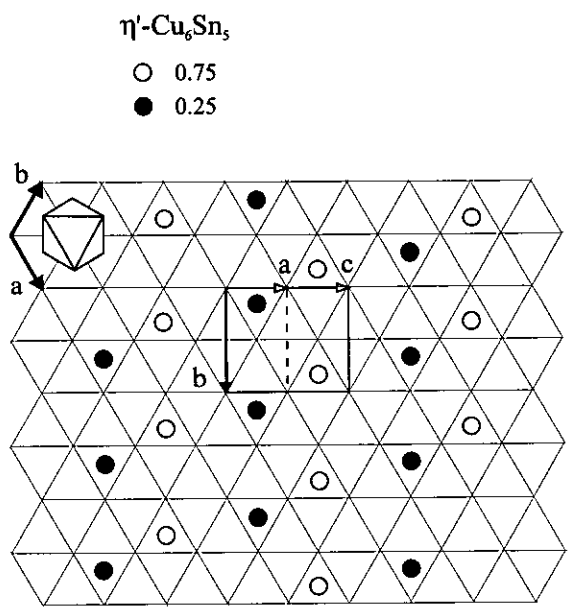

FIG. 7. η'-Cu_6Sn_5, projection along $22\bar{1}$*. The repeat distance along the c-axis in $B8$ is quintupled. The occupied positions corresponding to $2d$ in $B8_1$–$B8_2$ form sparse lines along the monoclinic b-axis at the heights 1/4, 3/4, . . . , 19/4, in units of the $B8$ c axis.

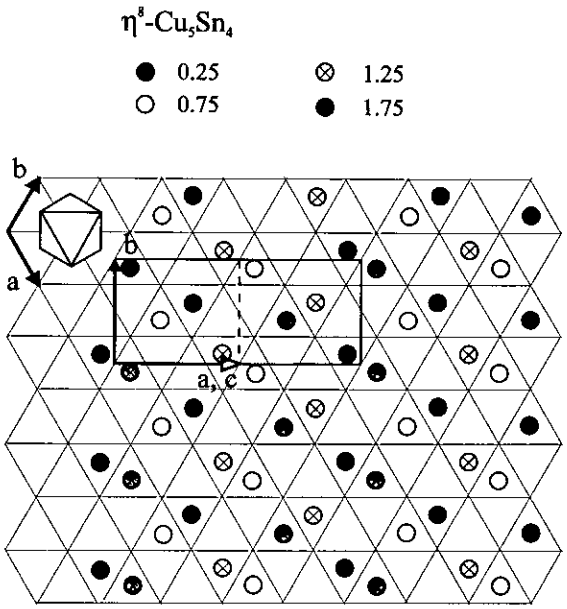

FIG. 8. η^8-Cu_5Sn_4, projection along $10\bar{1}$*. The repeat distance along the c-axis in $B8$ is doubled. The occupied positions corresponding to $2d$ in $B8_1$–$B8_2$ form an irregular grid in the hexagonal ab-plane. The positions constitute a subset (exactly half) of the positions in Ni_3Sn_2.

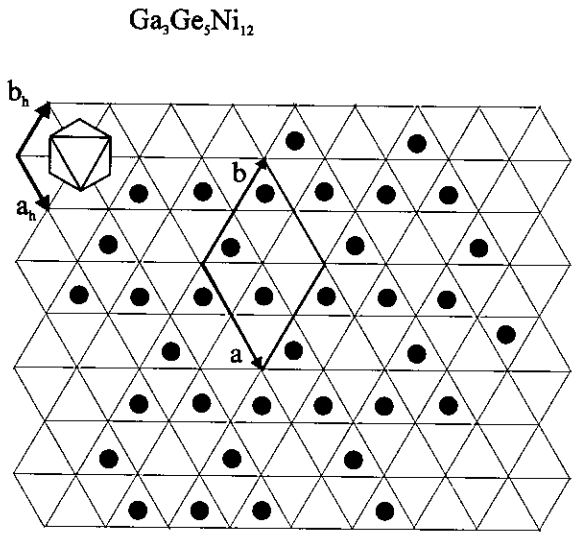

FIG. 10. $Ga_3Ge_6Ni_{12}$, bounded projection along 001*. The repeat distance along the c-axis in $B8$ is tripled. The occupied positions corresponding to $2d$ in $B8_1$–$B8_2$ form Kagomé nets at the heights 1/4, 3/4, 5/4, 7/4, 9/4, and 11/4 in units of the $B8$ c-axis.

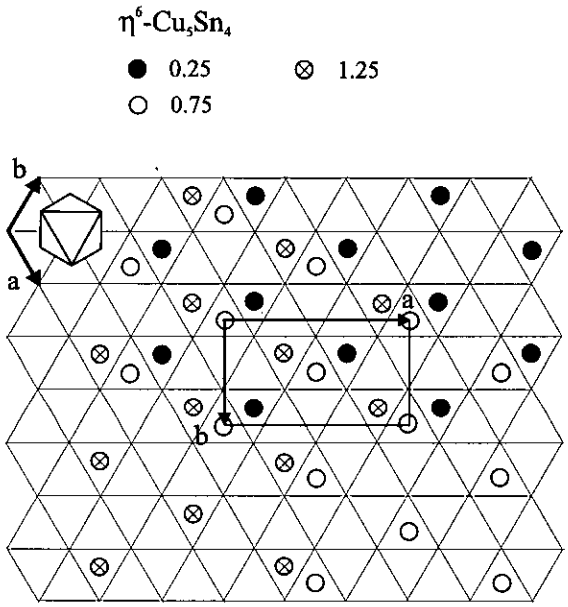

FIG. 9. η^6-Cu_5Sn_4, projection along 001*. The repeat distance along the c-axis in $B8$ is doubled. The occupied positions corresponding to $2d$ in $B8_1$–$B8_2$ form 6^3-nets at the heights 1/4, 5/4, and 7/4 in units of the $B8$ c-axis. The level corresponding to 3/4 is empty.

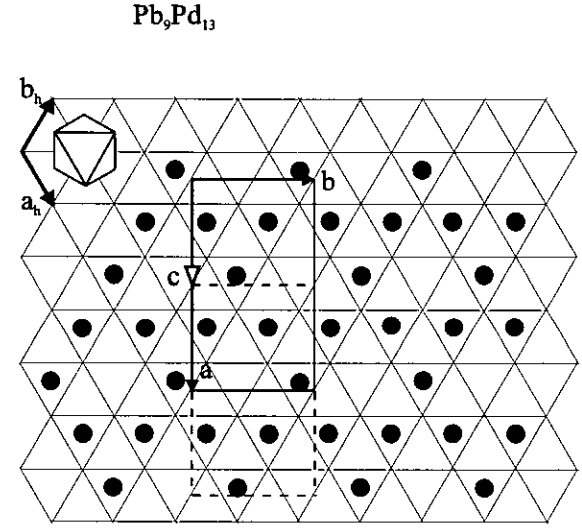

FIG. 11. Pb_9Pd_{13}, bounded projection along 001*. The repeat distance along the c-axis in $B8$ is quadrupled. The occupied positions corresponding to $2d$ in $B8_1$–$B8_2$ form Kagomé nets at the heights 1/4, 3/4, 5/4, 7/4, 9/4, 11/4, 13/4, and 15/4 in units of the $B8$ c-axis.

*B*8 lattice. An octahedron is indicated having the 2(*c*) positions for vertices and the 2*a* position as a center.

Coordinate table 1 In_3Pt_4 C2/m Shift=(0 1/4 0) Volume=8 x V_{Ni2In}

Atom	Wyckoff		x	y	z	Occ	Corresponding Ni_2In		Occ.
In1	2(d)	2/m	0.0	0.5	0.5	1.0	2(a)	{0.000 0.500 0.500}	1/8
In2	4(i)	m	0.1767	0.0	0.7716	1.0	2(c)	{0.208 0.000 0.750}	1/4
In3	4(i)	m	0.7126	0.0	0.7524	1.0	2(c)	{0.708 0.000 0.750}	1/4
In4	8(j)	1	0.9605	0.2124	0.7663	1.0	2(c)	{0.958 0.250 0.750}	1/2
Pt1	2(c)	2/m	0.0	0.0	0.5	1.0	2(a)	{0.000 0.000 0.500}	1/8
Pt2	4(f)	1	0.25	0.25	0.5	1.0	2(a)	{0.250 0.250 0.500}	1/4
Pt3	4(g)	2	0.0	0.2529	0.0	1.0	2(a)	{0.000 0.250 0.000}	1/4
Pt4	4(i)	m	0.4510	0.0	0.2719	1.0	2(d)	{0.458 0.000 0.250}	1/4
Pt5	4(i)	m	0.2582	0.0	0.9883	1.0	2(a)	{0.250 0.000 0.000}	1/4
Pt6	8(j)	1	0.8022	0.2570	0.7347	0.75	2(d)	{0.792 0.250 0.750}	3/8

Accumulated occupancy in the Ni_2In cell: a = 1, c = 1, d = 5/8;

Coordinate table 2 $Pd_{13}Tl_9$ $P\bar{3}m1$ Shift=(0 0 0) Volume=4 x V_{Ni2In}

Atom	Wyckoff		x	y	z	Occ	Corresponding Ni_2In pos.		Occ.
Pd1	1(a)	3m	0.0	0.0	0.0	1.0	2(a)	{0.000 0.000 0.000}	1/8
Pd2	3(e)	2/m	0.5	0.0	0.0	1.0	2(a)	{0.500 0.000 0.000}	3/8
Pd3	3(f)	2/m	0.5	0.0	0.5	1.0	2(a)	{0.500 0.000 0.500}	3/8
Pd4	6(i)	m	0.172	0.828	0.75	1.0	2(d)	{0.167 0.833 0.750}	3/4
Tl1	1(b)	3m	0.0	0.0	0.5	1.0	2(a)	{0.000 0.000 0.500}	1/8
Tl2	2(d)	3m	0.33	0.67	0.75	1.0	2(c)	{0.000 0.500 0.500}	1/4
Tl3	6(i)	m	0.202	0.798	0.25	1.0	2(c)	{0.167 0.833 0.250}	3/4

Accumulated occupancy in the Ni_2In cell: a = 1, c = 1, d = 3/4

Coordinate table 3 $Fe_{13}Ge_8$ $P6_3/mmc$ Shift=(0 0 0) Volume=4 x V_{Ni2In}

Atom	Wyckoff		x	y	z	Occ	Corresponding Ni_2In pos.		Occ.
Fe1	2(a)	3m	0.0	0.0	0.0	1.0	2(a)	{0.000 0.000 0.000}	1/4
Fe2	6(g)	2/m	0.5	0.0	0.0	1.0	2(a)	{0.500 0.000 0.000}	3/4
Fe3	6(h)	mm	0.8385	0.6770	0.25	0.83	2(d)	{0.833 0.667 0.250}	5/8
Ge1	2(d)	6m2	0.3333	0.6667	0.75	1.0	2(c)	{0.333 0.667 0.750}	1/4
Ge2	6(h)	mm	0.1922	0.3844	0.25	1.0	2(c)	{0.167 0.333 0.250}	3/4

Accumulated occupancy in the Ni_2In cell: a = 1, c = 1, d = 5/8

Coordinate table 4 $Ge_{12}Ni_{19}$ C2 Shift=(1/6 -1/6 1/8) Volume=12 x V_{Ni2In}

Atom	Wyckoff		x	y	z	Occ	Corresponding Ni_2In pos.		Occ.
Ge1	2(a)	2	0.0	0.019	0.0	1.0	2(c)	{0.000 0.000 0.000}	1/12
Ge2	2(b)	2	0.0	0.980	0.5	1.0	2(c)	{0.000 0.000 0.500}	1/12
Ge3	4(c)	1	0.012	0.339	0.25	1.0	2(c)	{0.000 0.333 0.250}	1/6
Ge4	4(c)	1	0.337	0.994	0.002	1.0	2(c)	{0.333 0.000 0.000}	1/6
Ge5	4(c)	1	0.334	0.015	0.496	1.0	2(c)	{0.333 0.000 0.500}	1/6
Ge6	4(c)	1	0.327	0.359	0.250	1.0	2(c)	{0.333 0.333 0.250}	1/6
Ge7	4(c)	1	0.337	0.317	0.748	1.0	2(c)	{0.333 0.333 0.750}	1/6
Ni1	2(b)	2	0.0	0.321	0.5	1.0	2(d)	{0.000 0.333 0.500}	1/12
Ni2	4(c)	1	0.997	0.989	0.246	1.0	2(d)	{0.000 0.000 0.250}	1/6
Ni3	4(c)	1	0.334	0.985	0.251	1.0	2(d)	{0.333 0.000 0.250}	1/6
Ni4	4(c)	1	0.341	0.310	0.010	1.0	2(d)	{0.333 0.333 0.000}	1/6
Ni5	4(c)	1	0.153	0.170	0.128	1.0	2(a)	{0.167 0.167 0.125}	1/6
Ni6	4(c)	1	0.158	0.142	0.379	1.0	2(a)	{0.167 0.167 0.375}	1/6
Ni7	4(c)	1	0.172	0.170	0.632	1.0	2(a)	{0.167 0.167 0.625}	1/6
Ni8	4(c)	1	0.186	0.187	0.875	1.0	2(a)	{0.167 0.167 0.875}	1/6
Ni9	4(c)	1	0.511	0.149	0.120	1.0	2(a)	{0.500 0.167 0.125}	1/6
Ni10	4(c)	1	0.519	0.184	0.372	1.0	2(a)	{0.500 0.167 0.375}	1/6

Accumulated occupancy in the Ni_2In cell: a = 1, c = 1, d = 7/12

Coordinate table 5 Ge_3Ni_5 C2 Shift=(1/12 1/6 1/4) Volume=6 x V_{Ni2In}

Atom	Wyckoff		x	y	z	Occ	Corresponding Ni_2In pos.		Occ.
Ge1	2(a)	2	0.0	0.039	0.0	1.0	2(c)	{0.000 0.000 0.000}	1/6
Ge2	2(b)	2	0.0	0.827	0.5	1.0	2(c)	{0.000 0.833 0.500}	1/6
Ge3	4(c)	1	0.352	0.983	0.996	1.0	2(c)	{0.333 0.000 0.000}	1/3
Ge4	4(c)	1	0.167	0.352	0.493	1.0	2(c)	{0.167 0.333 0.500}	1/3
Ni1	4(c)	1	0.070	0.170	0.252	1.0	2(a)	{0.083 0.167 0.250}	1/3
Ni2	4(c)	1	0.416	0.157	0.256	1.0	2(a)	{0.417 0.167 0.250}	1/3
Ni3	4(c)	1	0.771	0.179	0.255	1.0	2(a)	{0.750 0.167 0.250}	1/3
Ni4	4(c)	1	0.157	0.993	0.496	1.0	2(d)	{0.167 0.000 0.500}	1/3
Ni5	4(c)	1	0.323	0.322	0.009	1.0	2(d)	{0.333 0.333 0.000}	1/3

Accumulated occupancy in the Ni_2In cell: a = 1, c = 1, d = 2/3

Coordinate table 6 Ni_3Sn_2 Pnma Shift=(1/4 0 -1/8) Volume=4 x V_{Ni2In}

Atom	Wyckoff		x	y	z	Occ	Corresponding Ni_2In pos.		Occ.
Ni1	4(c)	m	0.919	0.25	0.878	1.0	2(d)	{0.917 0.250 0.875}	1/2
Ni2	8(d)	1	0.240	0.006	0.877	1.0	2(a)	{0.250 0.000 0.875}	1
Sn1	4(c)	m	0.602	0.25	0.360	1.0	2(c)	{0.575 0.250 0.375}	1/2
Sn2	4(c)	m	0.563	0.25	0.895	1.0	2(c)	{0.575 0.250 0.875}	1/2

Accumulated occupancy in the Ni_2In cell: a = 1, c = 1, d = 1/2

Coordinate table 7 η'-Cu_6Sn_5 C2/c Shift=(0 0 0) Volume=10 x V_{Ni2In}

Atom	Wyckoff		x	y	z	Occ	Corresponding Ni_2In pos.		Occ.
Sn1	8(f)	1	0.391	0.162	0.529	1.0	2(c)	{0.400 0.167 0.550}	2/5
Sn2	8(f)	1	0.285	0.655	0.358	1.0	2(c)	{0.300 0.667 0.350}	2/5
Sn3	4(e)	2	0.000	0.799	0.250	1.0	2(c)	{0.000 0:833 0.250}	1/5
Cu1	8(f)	1	0.101	0.473	0.202	1.0	2(a)	{0.100 0.500 0.200}	2/5
Cu2	8(f)	1	0.306	0.504	0.610	1.0	2(a)	{0.300 0.500 0.600}	2/5
Cu3	4(a)	1	0.000	0.000	0.000	1.0	2(a)	{0.000 0.000 0.000}	1/5
Cu4	4(e)	2	0.000	0.160	0.250	1.0	2(d)	{0.000 0.167 0.250}	1/5

Accumulated occupancy in the Ni_2In cell: a = 1, c = 1, d = 1/5

Coordinate table 8 η^8-Cu_5Sn_4 $P2_1/c$ Shift=(1/16 3/4 1/16) Volume=8 x V_{Ni2In}

Atom	Wyckoff		x	y	z	Occ	Corresponding Ni_2In pos.		Occ.
Sn1	4(e)	1	0.071	0.597	0.287	1.0	2(c)	{0.062 0.583 0.312}	1/4
Sn2	4(e)	1	0.180	0.057	0.440	1.0	2(c)	{0.188 0.083 0.437}	1/4
Sn3	4(e)	1	0.313	0.590	0.583	1.0	2(c)	{0.312 0.583 0.562}	1/4
Sn4	4(e)	1	0.451	0.087	0.663	1.0	2(c)	{0.438 0.083 0.687}	1/4
Cu1	4(e)	1	0.057	0.779	0.056	1.0	2(a)	{0.062 0.750 0.062}	1/4
Cu2	4(e)	1	0.189	0.253	0.187	1.0	2(a)	{0.188 0.250 0.187}	1/4
Cu3	4(e)	1	0.317	0.725	0.321	1.0	2(a)	{0.312 0.750 0.312}	1/4
Cu4	4(e)	1	0.427	0.258	0.427	1.0	2(a)	{0.438 0.250 0.437}	1/4
Cu5	4(e)	1	0.188	0.090	0.937	1.0	2(d)	{0.188 0.083 0.937}	1/4

Accumulated occupancy in the Ni_2In cell: a = 1, c = 1, d = 1/4

Coordinate table 9 η^6-Cu_5Sn_4 C2 Shift=(0 0 1/8) Volume=12 x V_{Ni2In}

Atom	Wyckoff		x	y	z	Occ	Corresponding Ni_2In pos.		Occ.
Sn1	2(a)	1	0.000	0.333	0.000	1.0	2(c)	{0.000 0.333 0.000}	1/12
Sn2	4(c)	1	0.307	0.349	0.009	1.0	2(c)	{0.333 0.333 0.000}	1/6
Sn3	4(c)	1	0.339	0.352	0.477	1.0	2(c)	{0.333 0.333 0.500}	1/6
Sn4	2(b)	1	0.000	0.360	0.000	1.0	2(c)	{0.000 0.333 0.500}	1/12
Sn5	4(c)	1	0.179	0.210	0.249	1.0	2(c)	{0.167 0.167 0.250}	1/6
Sn6	4(c)	1	0.488	0.190	0.268	1.0	2(c)	{0.500 0.167 0.250}	1/6
Sn7	4(c)	1	0.845	0.164	0.240	1.0	2(c)	{0.833 0.167 0.250}	1/6
Cu1	4(c)	1	0.022	0.007	0.127	1.0	2(a)	{0.000 0.000 0.125}	1/6
Cu2	4(c)	1	0.343	0.017	0.129	1.0	2(a)	{0.333 0.000 0.125}	1/6
Cu3	4(c)	1	0.653	0.034	0.133	1.0	2(a)	{0.667 0.000 0.125}	1/6
Cu4	4(c)	1	0.015	0.030	0.374	1.0	2(a)	{0.000 0.000 0.375}	1/6
Cu5	4(c)	1	0.326	0.000	0.379	1.0	2(a)	{0.333 0.000 0.375}	1/6
Cu6	4(c)	1	0.666	0.036	0.379	1.0	2(a)	{0.667 0.000 0.375}	1/6
Cu7	2(a)	1	0.000	0.691	0.000	1.0	2(d)	{0.000 0.667 0.000}	1/12
Cu8	4(c)	1	0.173	0.853	0.254	1.0	2(d)	{0.167 0.833 0.250}	1/6

Accumulated occupancy in the Ni_2In cell: a = 1, c = 1, d = 1/4

Coordinate table 10 $Ga_3Ge_6Ni_{12}$ $P3_121$ Shift=(0 0 0) Volume=12 x V_{Ni2In}

Atom	Wyckoff		x	y	z	Occ	Corresponding Ni_2In pos.		Occ.
M1	3(b)	2	0.498	0.0	0.833	1.0	2(a)	{0.500 0.000 0.833}	1/8
M2	6(c)	1	0.621	0.307	0.078	1.0	2(c)	{0.667 0.333 0.083}	1/4
M3	6(c)	1	0.313	0.194	0.921	1.0	2(c)	{0.333 0.167 0.917}	1/4
M4	6(c)	1	0.335	0.165	0.252	1.0	2(c)	{0.333 0.167 0.250}	1/4
M5	6(c)	1	0.309	0.120	0.589	1.0	2(c)	{0.333 0.167 0.583}	1/4
Ni1	3(a)	2	0.004	0.0	0.33	7/8	2(a)	{0.000 0.000 0.333}	7/64
Ni2	3(a)	2	0.492	0.0	0.33	7/8	2(a)	{0.500 0.000 0.333}	7/64
Ni3	3(a)	2	0.002	0.0	0.83	7/8	2(a)	{0.000 0.000 0.833}	7/64
Ni4	6(c)	1	0.493	0.995	0.99	7/8	2(a)	{0.500 0.000 0.000}	7/32
Ni5	6(c)	1	0.498	0.003	0.166	7/8	2(a)	{0.500 0.000 0.167}	7/32
Ni6	6(c)	1	0.680	0.333	0.247	7/8	2(d)	{0.667 0.333 0.250}	7/32
Ni7	6(c)	1	0.331	0.173	0.424	7/8	2(d)	{0.333 0.167 0.417}	7/32
Ni8	6(c)	1	0.342	0.169	0.752	7/8	2(d)	{0.333 0.167 0.750}	7/32

Accumulated occupancy in the Ni_2In cell: a = 57/64, c = 1, d =21/32.
Note that the composition of the compound does not agree with the structural determination.

Coordinate table 11 Pb_9Pd_{13} C2/c Shift=(0 0.125 0.25) Volume=16 x V_{Ni2In}

Atom	Wyckoff		x	y	z	Occ	Corresponding Ni_2In pos.		Occ.
Pb1	4(e)	2	0.0	0.8735	0.25	1.0	2(a)	{0.000 0.875 0.250}	1/8
Pb2	8(f)	1	0.4689	0.6645	0.1139	1.0	2(c)	{0.479 0.625 0.125}	1/4
Pb3	8(f)	1	0.4647	0.0805	0.1251	1.0	2(c)	{0.479 0.125 0.125}	1/4
Pb4	8(f)	1	0.2340	0.3768	0.1174	1.0	2(c)	{0.229 0.375 0.125}	1/4
Pb5	8(f)	1	0.2614	0.8717	0.1181	1.0	2(c)	{0.229 0.875 0.125}	1/4
Pd1	4(e)	2	0.0	0.3751	0.25	1.0	2(a)	{0.000 0.375 0.250}	1/8
Pd2	8(f)	1	0.1257	0.1125	0.5064	1.0	2(a)	{0.125 0.125 0.500}	1/4
Pd3	8(f)	1	0.3688	0.1316	0.0009	1.0	2(a)	{0.375 0.125 0.000}	1/4
Pd4	8(f)	1	0.1355	0.1171	0.1405	1.0	2(d)	{0.146 0.125 0.125}	1/4
Pd5	8(f)	1	0.0992	0.8732	0.3701	1.0	2(d)	{0.104 0.875 0.375}	1/4
Pd6	8(f)	1	0.2493	0.1239	0.2517	1.0	2(a)	{0.250 0.125 0.250}	1/4
Pd7	8(f)	1	0.1424	0.6345	0.1243	1.0	2(d)	{0.146 0.625 0.125}	1/4

Accumulated occupancy in the Ni_2In cell: a = 1, c = 1, d = 3/4

In some cases (In_3Pt_4, $Pd_{13}Tl_9$, $Ga_3Ge_6Ni_{12}$, and Pb_9Pd_{13}) the reported structures include some replacement of *T* atoms by *B* atoms. The structure types $Pd_{13}Tl_9$ and $Fe_{13}Ge_8$ are virtually identical, with the only significant difference being the partial occupancy in the latter. It is notable that each structure constitutes the most homogenous packing possible of the composition in the given space group. Structurally, it is convenient to group the superstructures into those in which the extra *T* atoms (corresponding to the 2(*d*) position in *B*8) form nets of hexagonal symmetry, and those where they do not. The latter case is the rarer; only in Ni_3Sn_2, η^8-Cu_5Sn_4 and η'-Cu_6Sn_5 do the extra atoms form other patterns.

CONCLUSIONS

The range of $B8_1$–$B8_2$ superstructures is very large indeed, and it is clear that the literature covers only a small part of it. There are nine reports of such structures that have not been solved. Some of these are suspect; the hexagonal Co_3Sn_2 may not exist at all (30), but we have found the system to contain other modulations in addition to that published. The two copper aluminides might be identical, but the systems Cu–Al, Cu–In, and Mn–Sn are the obvious choices for SAED–SXRD studies. Our experience from systems such as Cu–Sn and Co–Sn has been that a close-up, SAED look even at well-known systems is well worth the investigators' time.

APPENDIX

TABLE A1
Transformation Matrices for the Superstructure Cells

$$M_1 = \begin{bmatrix} 2 & 0 & 0 \\ 0 & 2 & 0 \\ 0 & 0 & 2 \end{bmatrix} \quad M_2 = \begin{bmatrix} 1 & \bar{1} & 0 \\ 1 & 1 & 0 \\ 0 & 0 & 2 \end{bmatrix} \quad M_3 = \begin{bmatrix} \bar{2} & 2 & 0 \\ 2 & 2 & 0 \\ \bar{1} & 1 & 1 \end{bmatrix}$$

$$M_4 = \begin{bmatrix} 8 & 8 & 0 \\ 1 & \bar{1} & 0 \\ 0 & 0 & 1 \end{bmatrix} \quad M_5 = \begin{bmatrix} 5 & 5 & 0 \\ 1 & \bar{1} & 0 \\ 0 & 0 & 1 \end{bmatrix} \quad M_6 = \begin{bmatrix} 2 & 0 & 0 \\ 0 & 2 & 0 \\ 0 & 0 & 1 \end{bmatrix}$$

$$M_7 = \begin{bmatrix} 0 & 0 & 2 \\ 2 & 2 & 0 \\ 1 & \bar{1} & 0 \end{bmatrix} \quad M_8 = \begin{bmatrix} 3 & 3 & 0 \\ \bar{1} & 1 & 0 \\ 0 & 0 & 2 \end{bmatrix} \quad M_9 = \begin{bmatrix} 3 & 3 & 0 \\ 1 & \bar{1} & 0 \\ 1 & 1 & \bar{1} \end{bmatrix}$$

$$M_{10} = \begin{bmatrix} 1 & \bar{1} & 0 \\ 0 & 0 & 1 \\ 2 & 2 & 0 \end{bmatrix} \quad M_{11} = \begin{bmatrix} 4 & 0 & 0 \\ 0 & 4 & 0 \\ 0 & 0 & 1 \end{bmatrix} \quad M_{12} = \begin{bmatrix} 1 & 1 & \bar{2} \\ \bar{1} & 1 & 0 \\ 2 & 2 & 1 \end{bmatrix}$$

TABLE A1—*Continued*

$$M_{13} = \begin{bmatrix} 2 & 2 & \bar{1} \\ \bar{1} & 1 & 0 \\ 2 & 2 & 1 \end{bmatrix} \qquad M_{14} = \begin{bmatrix} 3 & 0 & 0 \\ 0 & 3 & 0 \\ 0 & 0 & 1 \end{bmatrix} \qquad M_{15} = \begin{bmatrix} 2 & 0 & 0 \\ 0 & 2 & 0 \\ 0 & 0 & 3 \end{bmatrix}$$

$$M_{16} = \begin{bmatrix} 2 & \bar{2} & 0 \\ 2 & 2 & 0 \\ 1 & \bar{1} & 2 \end{bmatrix}$$

REFERENCES

1. P. Villars and L. D. Calvert (Eds.), "Pearsons Handbook of Crystallographic Data for Intermetallic Phases" ASM International, Material Park Ohio, 1992.
2. M. Hansen (Ed.), "Constitution of Binary Alloys" McGraw-Hill, New York, 1958.
3. "The Powder Diffraction File," JCPDS International Centre for Diffraction Data, 1992.
4. M. El-Boragy, R. Szepan, and K. Schubert, *J. Less-Common Met.* **29** 133 (1972).
5. G. D. Preston, *Philos. Mag.* **12,** 980 (1931).
6. A. J. Bradley, and P. Jones, *J. Inst. Met. London* **63,** 131 (1938).
7. S. Eymond, and E. Parthé, *J. Less-Common Met.* **19,** 441 (1969).
8. C. G. Wilson, *Acta Crystallogr.* **12,** 660 (1959).
9. M. Ellner, *J. Less-Common Met.* **48,** 21 (1976).
10. P. Feschotte, and P. Eggimann, *J. Less-Common Met.* **63,** 15 (1979).
11. M. Ellner, S. Bhan, and K. Schubert, *J. Less-Common Met.* **19,** 245 (1969).
12. T. A. Lobova, and T. A. Syrvacheva, *Sov. Powder Metall. Met. Ceram. Engl. Transl.* **244,** 321 (1983).
13. F. Laves, and H. J. Wallbaum, *Z. Angew. Mineral.* **4,** 17 (1942).
14. B. Bhattacharya, and D. B. Masson, *Mater. Sci. Eng.* **22,** 133 (1976).
15. P. Brand, *Z. Anorg. Allg. Chem.* **353,** 270 (1967).
16. S. Heinrich, and K. Schubert, *Z. Metallkd.* **69,** 230 (1978).
17. K. C. Jain, M. Ellner, and K. Schubert, *Z. Metallkd.* **62,** 456 (1973).
18. S. P. Yatsenko, A. A. Semyannikov, H. O. Shakarov, and E. G. Fedorova, *J. Less-Common Met.* **90,** 95 (1983).
19. R. R. Bitti, and V. Cascioli, *Scr. Metall.* **3,** 731 (1969).
20. G. Voss, *Z. Anorg. Allg. Chem.* **57,** 49 (1908).
21. W. B. Pearson, "Handbook of Lattice Spacings and Structures of Metals" Vol. 1, p. 813. 1958.
22. S. Bhan, T. Gödeke, P. K. Panday, and K. Schubert, *J. Less-Common Met.* **16,** 415 (1968).
23. S. Bhan, and K. Schubert, *Z. Metallkd.* **51,** 327 (1960).
24. B. Malaman, J. Steimetz, and B. Roques, *J. Less-Common Met.* **75,** 155 (1980).
25. M. Ellner, *J. Appl. Crystallogr.* **13,** 99 (1980).
26. M. Ellner, T. Gödeke, and K. Schubert, *J. Less-Common Met.* **24,** 23 (1971).
27. P. Brand, *Wiss. Z. Martin-Luther Univ. Halle-Wittenberg Math.-Naturwiss. Reihe* **16,** 551 (1967).
28. J. P. Jan, W. B. Pearson, A. Kjekshus, and S. B. Woods, *Can. J. Phys.* **41,** 2252 (1963).
29. H. Rajeswari, and H. Manohar, *Indian J. Pure Appl. Phys.* **8,** 363 (1970).
30. K. C. Jain, M. Ellner, and K. Schubert, *Z. Metallkd.* **63,** 258 (1972).
31. L. A. Panteleimonov, G. F. Portnova, and O. P. Nesterova, *Moscow Univ. Chem. Bull. Engl. Transl.* **26**(1), 79 (1971).
32. A.-K. Larsson, L. Stenberg, and S. Lidin, *Acta Crystallogr. Sect. B* **50,** 636 (1994).
33. A.-K. Larsson, L. Stenberg, and S. Lidin, submitted for publication.
34. M. Djega-Mariadassou, M. Both, and G. Trumpy, *Ann. Chim.* **5,** 505 (1970).
35. K. Yasukochi, and K. Kanematsu, *J. Phys. Soc. Jpn.* **16**(6), 1123 (1961).
36. H. Nowotny, K. Schubert, and U. Dettinger, *Z. Metallkd.* **37,** 137 (1946).
37. N. Sarah, K. Alasafi, and K. Schubert, *Z. Metallkd.* **72,** 517 (1981).
38. K. Schubert, *Z. Naturforsch. A* **2,** 120 (1947).
39. P. Pietrokowsky, and E. P. Frink, *Trans. Metall. Soc. AIME* **49,** 339 (1957).
40. R. R. Bitti, J. Diximier, and A. Guinier, *C. R. Hebd. Seances Acad. Sci. B* **266,** 565 (1968).
41. H. W. Mayer, M. Ellner, and K. Schubert, *J. Less-Common Met.* **71,** P29 (1980).
42. M. Ellner, T. Gödeke, and K. Schubert, *Z. Metallkd.* **64,** 566 (1973).
43. M. El-Boragy, K. C. Jain, H. W. Mayer, and K. Schubert, *Z. Metallkd.* **63,** 751 (1972).
44. L. F. Myzenkova, V. V. Baron, and E. M. Savitskii, *Russ. Metall. Engl. Transl.* **66**(2), 89.
45. H. Holseth, and A. Kjekshus, *Acta Chem. Scand.* **22,** 3273 (1968).
46. K. Schubert, H. G. Meissner, A. Raman, and W. Rossteutseher, *Naturwissenschaften* **51,** 287 (1964).
47. J. Bouwma, C. F. van Bruggen, and C. Haas, *J. Solid State Chem.* **7,** 255 (1973).
48. N. N. Zuravlev, G. S. Zdanov, and E. M. Smirnova, *Phys. Met. Metal.* **13**(4), 51 (1962).